Direct Voltammetric Investigation of the Electrochemical Properties of Human Hemoglobin: Relevance to Physiological Redox Chemistry†

Jeffrey I. Blankman,‡,§ Nazim Shahzad,‖ Cary J. Miller,*,⊥ and R. D. Guiles*,‖

Department of Chemistry and Biochemistry, University of Maryland, College Park, Maryland 20742, and Department of Pharmaceutical Sciences, University of Maryland, Baltimore, Maryland 21201

Received March 31, 2000; Revised Manuscript Received August 24, 2000

ABSTRACT: Voltammetric measurements on solutions of human hemoglobin using gold electrodes modified with ω-hydroxyalkanethiols have yielded the first direct measure of the reorganization energy of the protein. The value obtained based on extrapolation of the experimentally measured currents, 0.76 eV, is independent of pH (i.e., over the physiologically relevant rage, pH 6.8−7.4) and is remarkably similar to values obtained for myoglobin. This result is perhaps surprising given the marked dependence of the measured reduction potential of hemoglobin on pH (i.e., the redox Bohr effect). Electron transfer rates from the electrode to hemoglobin were also measured. Using similarly measured heterogeneous electron-transfer rates for cytochrome b_5, it is possible to predict the magnitude of the homogeneous electron-transfer rate from cytochrome b_5 to methemoglobin using a formalism developed by Marcus. These predicted rates are in reasonable agreement with reported rates of this physiological reaction based on stopped-flow kinetics experiments. These results suggest that the intrinsic electroreactivity of these heme proteins is sufficient to account for physiologically observed rates. Residual differences between homogeneous phase kinetics and those predicted by heterogeneous phase reactions are suggested to be due to small reductions in the outer-sphere reorganization energy of both component proteins which arise due to solvent exclusion at the interface between the two proteins in complex.

In our laboratories, Au electrodes modified with self-assembled ω-hydroxyalkanethiol monolayers have been used to control the reactivity of the electrode surface and have enabled the characterization of the electron-transfer properties of redox active heme proteins (*1*−*5*). These monolayers serve as electron tunneling barriers changing the absolute electron-transfer rate from the electrode to the redox centers in solution. By insulating an electrode with self-assembled ω-hydroxyalkanethiol monolayers, electrochemical characterizations become nearly as easy for the redox proteins as for small redox molecules (*4*, *5*).

A persistent difficulty experienced with the direct voltammetric measurements of proteins is electrode passivation. It has been seen that bare metal electrodes are quickly passivated by the nonspecific adsorption of the protein to the electrode surface, rendering the surface inactive (*4*, *5*). Voltammetric measurements of hemoglobin have been done with redox mediators (*6*, *7*) and surfactant films (*8*, *9*) and, recently, directly using lipoic acid (*11*) and L-cysteine monolayers on silver (*12*).

In this paper, we present the direct voltammetry of hemoglobin under physiological conditions (i.e., pH 6.8−7.4) using electrodes that are relatively free of artifacts due to electrode passivation and background currents (*1*, *2*, *12*). We have also compared the voltammetric behavior of hemoglobin to myoglobin under identical conditions. The redox Bohr effect (*13*, *14*), a shifting of the formal potential as a function of pH, is clearly evident in the direct voltammetry of hemoglobin. Surprisingly, the reorganization energies of these two oxygen-binding proteins are both relatively independent of pH despite significant differences in the measured reduction potential as a function of pH.

In this paper, we have also characterized the kinetic properties of hemoglobin electron transfer through the use of ω-hydroxyalkanethiol modified gold electrodes. Voltammetric studies of heme proteins can yield significant quantitative measures of the redox reactivity (*15*−*19*). The relevance of these kinetic parameters determined using metallic electrodes to measured homogeneous solution-phase kinetics is also discussed. Although comparisons between heterogeneous electron-transfer kinetics and homogeneous solution-phase kinetics have been performed for inorganic ions in solution (*20*−*22*), here we present the first detailed analysis of an interprotein electron-transfer reaction. To probe whether the intrinsic electroreactivity of hemoglobin and cytochrome b_5 is sufficient to account for rates of reduction of methemoglobin by cytochrome b_5 under physiologically relevant conditions, we have compared the electrode kinetics to previously determined homogeneous rates (*23*) using

† The generous support of the National Science Foundation (CHE 9417357 to C.J.M and MCB 9904422 to R.D.G.) is gratefully acknowledged.

* To whom correspondence should be addressed.

‡ Department of Chemistry and Biochemistry

§ Current address: Wyeth-Ayerst ESI Lederle, 2 Easterbrook Lane, Cherry Hill, NJ 08003.

‖ Department of Pharmaceutical Sciences.

⊥ Current address: i-Stat Corporation, 436 Hazeldean Road, Kanata, Canada K2L 1T9.

10.1021/bi000731b CCC: $19.00
Published on Web 11/03/2000

formalisms developed by Marcus (*24*, *25*). Our recent characterizations of the electrochemical properties of cytochrome b_5 (*26*, *27*) were another important contributor to our ability to perform these analyses. It is important to note that while comparisons between autoexchange rates of redox active proteins and cross-reaction rates between these proteins have been performed for many interprotein electron transfers, comparisons between heterogeneous electron-transfer rates determined from voltammetric measurements and cross-reaction rates determined in solution have not been performed (for a review of these topics, see ref *25*).

EXPERIMENTAL SECTION

Protein Purification. Hemoglobin (Human, Sigma) solutions (20 mM Tris and 1 mM EDTA,[1] pH 7.6 buffer) were reduced with sodium dithionite for enhanced stability. The solutions were further purified using a Sephacryl S-100-HR column (28 mm × 95 cm, Sigma). These solutions were then concentrated and passed over a DEAE anion-exchange column (5 mm × 8 cm, Sigma) and eluted with 50 mM Tris, 0.1 mM EDTA, pH 8.0 buffer. This solution was passed over a CM cellulose cation-exchange resin (5 mm × 8 cm, Sigma) and eluted with a gradient elution profile, 0.2−0.4 M NaCl. The resulting solution was dialyzed against 20 mM MOPS buffer (pH 7.4, Sigma) and concentrated using an Amicon filtration system (Millipore). The buffer solution was exchanged to the desired pH using MOPS, a noncoordinating buffer, instead of phosphate because of possible complications in the electrochemical measurements (*8*, *28*, *29*). Immediately prior to electrochemical measurements, hemoglobin samples were oxidized using potassium ferricyanide (Sigma) and passed over a Sephadex G-25 (28 mm × 17 cm, Sigma) column to remove residual ferri/ferrocyanide. All electrochemical measurements were performed using sodium trifluoroacetate (Sigma) as the electrolyte.

Electrode Preparation. The ω-hydroxyalkanethiols used were purchased from Aldrich, purified twice using silica column chromatography to remove any dithiols, and adsorbed onto freshly sputtered and cleaned Au electrodes (0.13 cm^2) as described previously (*5*). Reduction potential measurements were performed with surface-modified electrodes prepared from 3-mercapto-1-propanol. Voltammetric measurements used in the determination of kinetic parameters for hemoglobin were performed using surface modified electrodes prepared using 6-mercapto-1-hexanol. Voltammetric measurements previously used to measure kinetic parameters of cytochromes b_5 and *c* were performed using electrodes prepared using 11-mercapto-1-undecanol.

Electrochemical Measurements. All electrochemical experiments were performed in a jacketed electrochemical cell held at 0.0 °C, utilizing a Bioanalytical Systems BAS-100B potentiostat and Fisher Scientific model 9101 thermostat. A standard three-electrode cell was used with a Pt counter electrode, and all measurements are reported versus a saturated calomel reference electrode (SCE). All solutions were held under a N_2 atmosphere during the electrochemical experiments. The concentration of each solution was determined by optical spectroscopy immediately prior to and following kinetic experiments. Extinction coefficients used in the determination of the concentration of methemoglobin (pH 6.4) were 179 mM^{-1} at 409 nm and 188 mM^{-1} at 408 nm for metmyoglobin (pH 6.4) (*31*).

[1] Abbreviations: DEAE, diethyl amino ethyl (cellulose); EDTA, ethylenediaminetetraacetic acid; CM, carboxymethyl (cellulose); MOPS, 3-[*N*-morpholino]propanesulfonic acid; SCE, saturated calomel electrode.

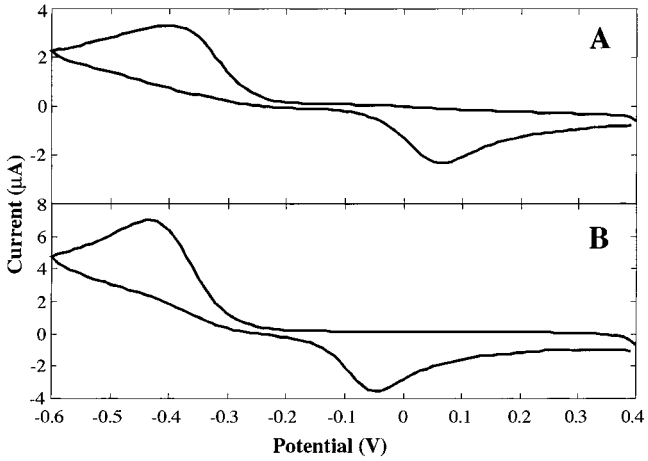

FIGURE 1: Cyclic voltammograms of (A) 0.25 mM hemoglobin and (B) 1.5 mM myoglobin on gold electrodes derivatized with 3-mercapto-1-propanol. Solutions were in 10 mM MOPS, 0.375 M NaTFA, pH 7.1, at 50 mV/s. The temperature of the cell was held at 0.0 °C. Potentials are reported versus the saturated calomel electrode. The electrode area was 0.13 cm^2.

RESULTS

Measurement of Reduction Potentials. The use of Au electrodes that have been insulated with ω-hydroxyalkanethiol monolayers has allowed our group to perform direct voltammetric measurements of protein solutions. The quasi-reversible voltammograms of hemoglobin and myoglobin are remarkably similar. Typical voltammograms of human hemoglobin and, for comparison, horse myoglobin, recorded using short chain length ω-hydroxyalkanethiols, are shown in Figure 1. Reduction potentials are easily and accurately determined from these voltammograms. By contrast, the voltammetry of these proteins using bare gold electrodes yields voltammetric currents which lack any observable faradaic component. As has been previously observed for both myoglobin (*32*) and hemoglobin (*8*, *11*) the peak of the cathodic wave in the voltammogram of hemoglobin shifts to more negative potentials with increasing scan rate. The cathodic peak potential shifts 74 ± 4 mV more negative at 200 mV/s relative to slower scan rates shown in Figures 1 and 4 (i.e., 50 and 100 mV/sec, respectively).

Determination of Kinetic Parameters. The use of ω-hydroxyalkanethiol monolayers with longer hydrocarbon chain lengths allow one to measure the heterogeneous electron-transfer kinetics of small molecules and redox proteins. The corrected currents (i.e., corrected for residual diffusion controlled currents and electric double layer effects) are normalized to unit electrode area and redox concentration to give heterogeneous electron-transfer rates as a function of formal overpotentials. Using $HO(CH_2)_6SH$-coated electrodes, we find the heterogeneous electron transfer rates are decreased sufficiently to allow their measurement over the accessible voltammetric range of the insulated electrode. Representative voltammograms observed for hemoglobin and myoglobin using these longer chain monolayers can be seen in Figure 2.

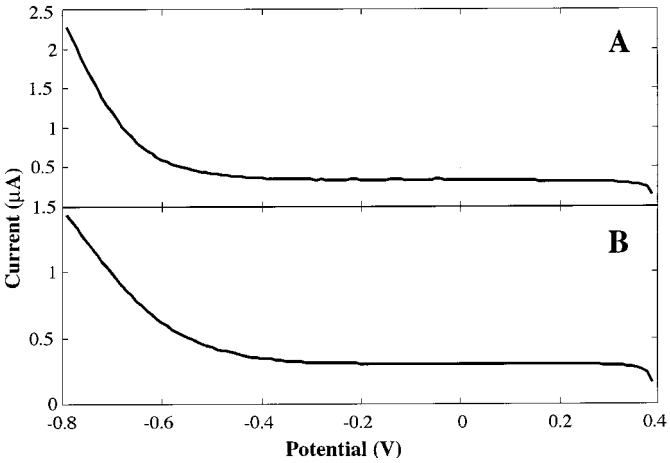

FIGURE 2: Linear sweep voltammograms recorded under cyclic voltammetric conditions for the two solutions from Figure 1 using gold electrodes derivatized with 6-mercapto-1-hexanol. Voltammograms were recorded at 5.12 V/s, 0.0 °C, and reported versus the saturated calomel electrode. The electrode area was 0.13 cm^2.

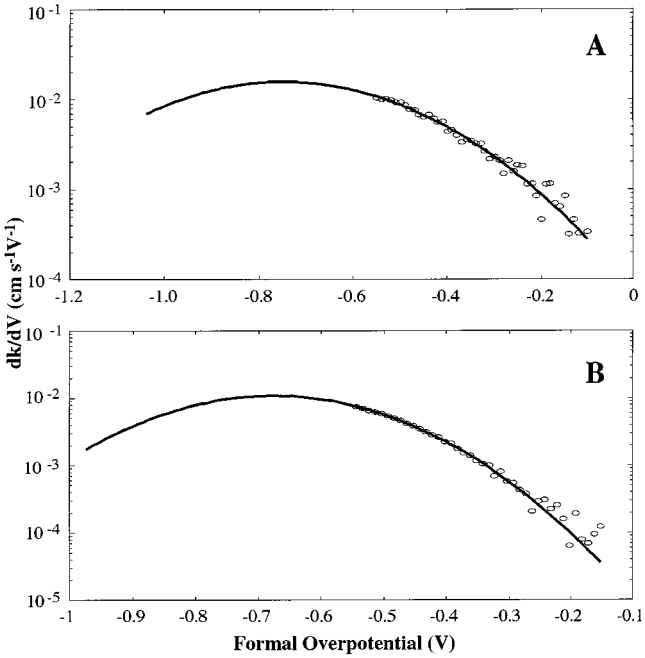

FIGURE 3: Plots of the potential derivative of the heterogeneous electron-transfer rate constants for the heme proteins derived from the data in Figure 2. These derivative plots are proportional to the density of electronic states distributions within the redox species at the electrode surface. The solid curves represent the best fit Gaussian to the experimental points.

The analysis of voltammograms employing longer length monolayers enable one to separate the activation and electronic coupling components of the redox protein's reactivity. The reorganization energy is obtained as the peak of the Gaussian curve obtained by fitting the derivative of the current versus applied potential data while estimates of the electronic coupling are determined from limiting heterogeneous rate constants determined from the integration of the fitted curve as described in detail below. The current for the reduction of the redox species is corrected for diffusion limitations and electrostatic double layer effects as previously described (*1*, *2*, *12*). The diffusion coefficients and effective charges are collected in Table 1.

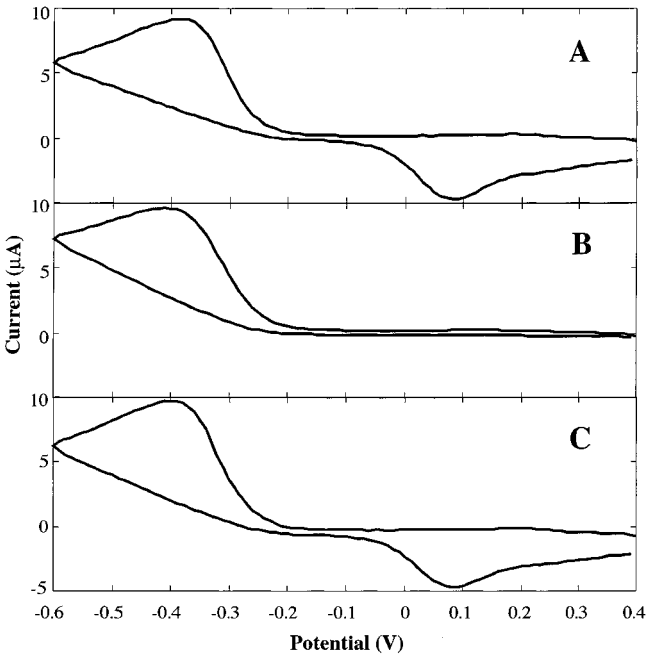

FIGURE 4: Cyclic voltammograms of 0.5 mM hemoglobin in 10 mM MOPS, 0.375 M NaTFA, pH 6.8, (A) without oxygen, (B) in the presence of oxygen, and (C) repurged of oxygen. All voltammograms were recorded at 100 mV/s, 0.0 °C, and reported versus the saturated calomel electrode. The electrode area was 0.13 cm^2.

Table 1: Diffusion Coefficients, Effective Charges, and Percent Active Surface Areas

protein	D_o[a] ($\times 10^7$ cm^2/s)	Z_{eff}[b]	active surface area percent[c]
myoglobin	7.5 ± 0.8	0.6 ± 0.2	1.9
hemoglobin	3.4 ± 0.7	0.6 ± 0.3	3.4
cytochrome b_5	3.8 ± 0.8	-1.4 ± 0.5	3.5

[a] Diffusion coefficients were determined at 0.0 °C. The reported uncertainties are standard deviations from repeated measurements. [b] The effective charge for the proteins were calculated by changing the ionic strength of the solutions from 0.05−0.80 M at 0.0 °C and the heterogeneous electron-transfer rate constants were measured at $HO(CH_2)_6SH$ electrodes. The diffuse layer potential was calculated at both ionic strengths and the effective charge was determined. [c] The active surface area percent was calculated by determining the water-accessible surface of the heme divided by the water accessible surface of the entire protein (*47*). This relative surface was used in correcting measured heterogeneous rates (eqs 8 and 9).

The potential derivative of the electron-transfer rate is proportional to the density of electronic states distribution for the redox species. Figure 3 shows representative density of electronic states distributions for hemoglobin. The solid line is the best fit Gaussian which is predicted by the Marcus theory (*24*, *33*). The position of the peak of the density of states, obtained by extrapolation of the data due to the limited voltammetric range, gives a measure of the reorganization energy, λ. The reorganization energies of hemoglobin and myoglobin determined from these insulated electrodes are collected in Table 2.

The density of electronic states distribution can also yield a measure of the electronic coupling between the electrode and the redox species. The maximum heterogeneous electron-transfer rate, k_{max}, can be obtained as the area under the density of electronic states curve. The electron transfer rate depends mostly on the probability of electron tunneling from the electrode to the redox site. In addition, the k_{max} parameter

Table 2: Formal Potentials, Reorganization Energies, and k_{max} Values for Hemoglobin and Myoglobin at Biologically Relevant pHs

protein	$E^{\circ\prime}$ [a] (V vs SCE)	λ [b] (eV)	k_{max} [b] (cm/s)
hemoglobin			
pH 6.8	-0.156 ± 0.005	0.76 ± 0.02	0.012 ± 0.002
pH 7.1	-0.170 ± 0.004	0.76 ± 0.04	0.014 ± 0.005
pH 7.4	-0.192 ± 0.005	0.78 ± 0.06	0.011 ± 0.005
myoglobin			
pH 6.8	-0.240 ± 0.005	0.70 ± 0.02	0.0043 ± 0.0002
pH 7.1	-0.235 ± 0.004	0.72 ± 0.02	0.0039 ± 0.0004
pH 7.4	-0.238 ± 0.004	0.71 ± 0.01	0.0038 ± 0.0003
cytochrome b_5 [c]	-0.212 ± 0.002	0.44 ± 0.02	$0.000\,40 \pm 0.000\,10$

[a] The formal potential was measured as the average of the cathodic and anodic peak potentials. [b] The reported uncertainties are standard deviations from at least eight replicate measurements. [c] Cytochrome b_5 measurements were all performed in 10 mM MOPS buffer, pH 7.1, with 0.375 M NaTFA at 0 °C using gold electrodes modified with 11-mercapto-1-undecanol.

reflects the number of reactive redox molecules within the reaction layer at the electrode surface. The k_{max} values determined for hemoglobin and myoglobin are listed in Table 2.

An extremely important term involved in the electrostatic double layer correction is the effective charge of the protein. The effective charge is not the overall charge of the protein, but the local charge at the redox site. This parameter is calculated using kinetically limited currents measured at two ionic strengths, as previously described (*5*). For these protein solutions, the ionic strengths used were 0.050 and 0.80 M. The diffusion coefficients were determined using chronocoulometry. Values for the diffusion coefficients and effective charges are collected in Table 1.

Calculation of the Homogeneous Electron-Transfer Rate Constant from Measured Heterogeneous Rates. The electron-transfer kinetics of a homogeneous cross-reaction can be compared to the kinetics of the individual electrode half-reactions (*20*−*22*, *25*). Marcus theory (*25*) predicts the relationship between these reactions to be

$$\frac{k^{e}_{AB}}{Z_e} = \left(\frac{k^{h}_{AB}}{Z_h}\right)^{1/2} \tag{1}$$

where k^{h}_{AB} is the homogeneous electron-transfer rate, k^{e}_{AB} is the heterogeneous electron-transfer rate, Z_e and Z_h are the electrochemical and homogeneous collisional frequencies respectively (*21*).

For the oxidation−reduction reaction (*20*),

$$A_1 + B_2 \rightarrow A_2 + B_1 \tag{2a}$$

one can associate the following electrochemical reactions:

$$A_1 + e^- \rightarrow A_2 \tag{2b}$$

$$B_2 \rightarrow B_1 + e^- \tag{2c}$$

The rate constant for the electrochemical reactions can be written according to Marcus theory (*25*) at overpotentials where the double-layer terms are negligible (*20*).

Using this theory, the following arguments can be made using experimentally determined parameters. In the experiments presented here, the diffusion-corrected current was corrected for double-layer effects prior to determination of the kinetics. The corrected current is normalized to unit electrode area and concentration to give the heterogeneous electron-transfer rate constants as a function of the formal overpotential. Rate constants for the reduction of A at the formal potential of A (i.e., k_A) were determined by extrapolation from rate constants determined at a potential more negative than the formal potential, and vice versa for the oxidation of B (i.e., k_B).

$$\ln k_A = \ln k^{s}_{A} - \frac{F}{2RT}(E - E^{\circ}_{A}) \tag{3a}$$

$$\ln k_B = \ln k^{s}_{B} + \frac{F}{2RT}(E - E^{\circ}_{B}) \tag{3b}$$

where E is the potential at which the rate constant is determined, E° is the formal potential of the redox species. The heterogeneous kinetics (i.e., k^{s}_{A} and k^{s}_{B}) determined at the reorganization potential allows substitution of λ into eqs 3a and 3b. The measured rate constants were determined using different length monolayers, and must be corrected to electrodes coated with monolayers containing equal length blocking ω-hydroxyalkanethiol monolayers. For the purpose of comparing the homogeneous kinetics, the electrode kinetics will be corrected to a bare gold electrode (i.e., equivalent to direct van der Waals contact with the gold surface), assuming a nonadiabatic reaction, using the following relationship (*2*, *5*):

$$k = k_{max} e^{\beta n} \tag{4}$$

where β is the tunneling decay coefficient, 1.08/methylene (*5*), and n is the number of methylene units in the monolayer. The k_{max} terms collected in Table 2 are determined from integration of the fitted density of states equation. The integral of the density of states distribution beyond 2λ is the maximum heterogeneous electron-transfer rate constant. Therefore, at the reorganization potential, the heterogeneous electron-transfer rate will be half of the k_{max}. Substitution of these values into eqs 3a and 3b yields

$$\ln k_A = \ln \frac{k^{0}_{max_A}}{2} - \frac{F}{2RT}(\lambda_{red}) \tag{5a}$$

$$\ln k_B = \ln \frac{k^{0}_{max_A}}{2} - \frac{F}{2RT}(-\lambda_{ox}) \tag{5b}$$

The results from eqs 5a and 5b are collected in Table 3.

Marcus has shown that the relationship between the rate constant for the homogeneous cross-reactions and the rate constants for heterogeneous rates determined voltammetrically are as follows (*20*−*22*, *25*):

$$\ln k_{AB} = 0.5(\ln k_A + \ln k_B + \ln K_{AB}) \tag{6}$$

where k_A and k_B are the corrected heterogeneous electron-transfer rate constants from eqs 5a and 5b, respectively, and K_{AB} is the equilibrium constant of reaction 2a.

$$\ln K_{AB} = \frac{F}{RT}(E^{\circ}_{red} - E^{\circ}_{ox}) \tag{7}$$

The results of these calculations are listed in Table 3.

Table 3: Heterogeneous Electron Transfer Kinetics and Predicted Homogeneous Solution Cross-Reaction Rates

protein	k_A^s [a]	k_A(corr) [b]	k_A [c]	k_{AB}^e [d]	k_{AB}^h [e]
cytochrome b_5	0.000 40	58	2.5×10^{-3}		
hemoglobin	0.014	9.1	4.4×10^{-7}		
cytochrome b_5−hemoglobin complex				8.1×10^{-5}	0.0021

[a] Limiting current using an 11-mercapto-1-undecanol monolayer for cytochrome b_5 and a 6-mercapto-1-hexanol monolayer for hemoglobin. [b] Rates are corrected to a bare gold electrode using eq 4. [c] Rates corrected to the reduction potential of the protein using eqs 5a and 5b. [d] Heterogeneous cross-reaction rates predicted by eq 6. [e] Homogeneous cross-reaction rates predicted by eq 1.

The collisional frequency of the protein with the electrode (*24*) including a steric factor defining the electroactive surface area (see Table 1) is given by

$$Z_e = \left(\frac{kT}{2\pi m_r}\right)^{1/2} \times S \tag{8}$$

where k is Boltzmann's constant, T is the absolute temperature, m_r is the reduced mass of the protein−protein complex, and S is the average electroactive surface area of the protein. The value of the heterogeneous collisional frequency was calculated to be 21 cm/s. The surface area is expressed as a ratio of the active surface area to the overall reaction surface area and is between 0 and 1, with one being 100% active surface area.

The collisional frequency of the homogeneous reaction (*24*) is given with the steric corrections for both protein components is given by

$$Z_h = N\left(\frac{8\pi kT}{m_r}\right)^{1/2} \frac{r^2}{10^3} S_A S_B \tag{9}$$

where N is Avogadro's number, m_r is the reduced mass of the protein−protein complex, r is the distance between the metal centers (in cm), S_A and S_B are the active surface areas of protein A and B, respectively. Modeling of the hemoglobin−cytochrome b_5 complex based largely on electrostatic interactions suggests an Fe−Fe distance of 16 Å (*34*). The homogeneous collisional frequency has a calculated value of 1.4×10^8 s^{-1}.

Using eq 1, the homogeneous electron-transfer rate constant calculated from measured heterogeneous electrode reaction rates yield 0.0072 s^{-1}. This value can be compared to a previously measured homogeneous rate constant. McLendon reported the homogeneous electron-transfer rate constant between these proteins at various temperatures (*23*). Extrapolation of these data yields the rate constant at 0 °C, 0.17 s^{-1}. This data was recorded in a pH 6.2 phosphate buffer solution. It has been shown that the homogeneous electron-transfer rate between metal-substituted hemoglobins and cytochrome b_5 is half at pH 7 than that observed at pH 6 (*35*). Taking this into account, the homogeneous rate constant at pH 7.1 would be approximately 0.08 s^{-1}. These values are collected in Table 4.

Before comparing the homogeneous rate constant from McLendon's work to the value calculated here, one must also correct the homogeneous rate data for the work associated with bringing the two charged proteins together. This correction has been used for both small redox molecules (*20*−*22*, *36*, *37*) as well as proteins (*38*−*44*). This correction is applied using a version of the Debye−Hückel equation (*21*, *25*, *45*)

Table 4: Homogeneous Cross-reaction Kinetics Extrapolated from Stopped-flow and Pulse-radiolysis Methods

	k_{AB}^h		
	pH 6.0 [a]	pH 7.1 [b]	corr [c]
cytochrome b_5−hemoglobin complex	0.17	0.08	0.037

[a] Rates measured by extrapolation of previously reported results to 0 °C. [b] Rates corrected to pH 7.1. [c] Rates corrected for electrostatic work term using eq 10.

$$\log k = \log k_{AB}^h + \frac{2Z_A Z_B A\sqrt{I}}{1+\sqrt{I}} \tag{10}$$

where Z_A and Z_B are the effective charges of the proteins, A is the Debye constant (0.51), and I is the ionic strength.

Through this correction, a homogeneous rate constant of 0.037 s^{-1} is calculated from the cross-reaction as compared to the 0.0021 s^{-1} calculated from the two corresponding heterogeneous electron-transfer rate constants.

Biological Activity of Hemoglobin. The electroreactivity of hemoglobin was tested in the absence and presence of oxygen. It can be seen from Figure 4 that in the absence of oxygen there are well-defined reduction and reoxidation waves. Upon introducing oxygen into the cell, the reoxidation wave is absent, as seen in Figure 4B. This is attributed to the binding of oxygen upon reduction of the protein (*46*). Blanketing the solution with nitrogen results in deoxygenation. This results in the return of the oxidative peak, as shown in Figure 4C. Similar observations in the voltammetry of myoglobin in the presence of oxygen have been reported previously (*32*).

The oxidation peak in the presence of oxygen is not necessarily absent, per se, but most likely has been shifted to much more positive potentials. The binding of oxygen to the metal center stabilizes the protein. It therefore is reasonable to assume that the oxidative wave has been shifted outside of the voltammetric window of these electrodes. The identical behavior has already been seen in myoglobin and was reconfirmed with these electrodes (*5*). It is quite common to see a shift in the formal potential of a molecule following a chemical reaction. An alternative, but much less likely explanation, is that there has been a large decrease in the electronic coupling to the electrode.

DISCUSSION

The use of ω-hydroxyalkanethiol monolayers has allowed the direct electrochemical measurement of the pH dependence of the reduction potential and heterogeneous electron transfer kinetic parameters of hemoglobin. The longer thiol monolayers allowed the elucidation and separation of thermodynamic and kinetic properties of the electron transfer. The reorganization energies, listed in Table 2, for hemoglobin

and myoglobin are nearly identical. These reorganization energies are only about 0.2 eV higher than those reported for cytochromes *c* and b_5 (*5*). The higher reorganization energy of hemoglobin has been attributed to the an increase in the inner sphere component of the reorganization energy consistent with the movement of the iron out of the plane of the heme upon reduction (*5*).

Comparisons between electronic coupling parameters, k_{max}, are less straightforward. On the basis of measured heterogeneous rates, normalized to unit concentration and electrode area, hemoglobin is three times more electroactive at the electrode surface than myoglobin. Because the length of the monolayer used to measure the kinetics was the same, $HO(CH_2)_6SH$, there is no need to correct for differences in the electron tunneling decay. However, the k_{max} parameter is also a measure of the number of reactive species at the electrode surface, and should be corrected for these differences. For small redox molecules, such as ferricyanide, all orientations of the roughly spherical molecule should be equally electroactive. When the proteins approach the electrode surface, only a small percentage of the molecules are oriented with the exposed edge of the heme facing the electrode. These electroactive surface area percentages (*47*) are listed in Table 1. The percentage of the protein surface which is electroreactive was estimated as follows. For hemoglobin, the central bis(phosphoglycerate) binding pocket was excluded because the inside of the pocket has no direct interaction with the surface of the electrode. The total solvent-accessible surface of the protein was calculated as described by Connolly (*47*) and the fraction of that surface containing exposed heme atoms was determined using the program *ms* which is distributed with the *MidasPlus* package (UCSF Computer Graphics Laboratory, San Francisco). Using this as the percentage of active molecules at the electrode surface, the hemoglobin electronically couples to the electrode surface better than myoglobin by a factor of 1.7.

Correcting the measured currents for differences in reactive surface area, the measured heterogeneous electron transfer rates are indistinguishable within the limits of uncertainty in the measurement. Both proteins share the ability to reversibly bind oxygen, and hemoglobin resembles a tetramer of myoglobins. Not surprisingly, the similarities in the kinetic and thermodynamic parameters for these proteins supports the similarities in structure and function.

Formal Potentials and the Redox Bohr Effect. A notable difference between the proteins is the position of the oxidative wave. In hemoglobin, the oxidation wave is shifted approximately 125 mV positive of the corresponding myoglobin wave. This large shift helps to stabilize the molecule in the reduced form, which is the biologically important oxidation state. Ferric hemoglobin and myoglobin do not bind oxygen, and are not biologically functional. Hence, it is physiologically important for these proteins to remain in the reduced form.

It can be seen from Table 2 that as the pH increases the formal potential of hemoglobin becomes more negative. These results agree with the previously reported trend in the direction of the formal potential shift (*46*). Observation of the pH dependence of the reduction potential [i.e., the Redox Bohr effect (*46*)] of hemoglobin illustrates the utility of direct voltammetric methods in the rapid evaluation of allosteric functionality of the hemoglobin sample. Myoglobin was a useful nonallosteric control. Recently, more extensive analyses of anion effects on allosteric and redox behavior of hemoglobin have been reported by Faulkner et al. (*29*) using spectroelectrochemistry.

Comparison between Calculated and Reported Homogeneous Electron-Transfer Rates. The fact that the homogeneous rate, following corrections for electrostatic work terms, is roughly 18 times greater than that determined from a calculation based on heterogeneous rates is actually fairly reasonable (i.e., 0.037 for the former versus 0.0021 for the latter). The difference between calculated rates based on heterogeneous electron-transfer rates and measured homogeneous rates may be due to effects induced by protein complex formation. Note that we have used the thermodynamic electromotive driving force for the estimation of the equilibrium constant used in eq 6. That is, we used potentials determined from voltammograms with slow scan rates (i.e., 50 mV/s). We observed a −72 mV shift in the peak potential of the cathodic wave at higher scan rates and the affect of this magnitude shift would have reduced the calculated estimate of the homogeneous electron-transfer rate, k^e_{AB} in Table 3, by a factor of 2.1. However, the negative shift of the cathodic wave is compensated for by a positive shift in the anodic wave resulting in a negligible shift in the reduction potential as a function of scan rate. Nonetheless, the non-Nernstian behavior of this reduction may be physiologically significant. The origins of this effect have been attributed to a slow dissociation of water following reduction (*8*,*32*). Thus, in principle, the reorganization energy may be effectively lowered by this slow dissociation, without changing the overall thermodynamic stabilization gained by the subsequent dissociation of the water from the ferrous protein.

There have been many arguments in the literature of interprotein electron-transfer kinetics which have suggested mechanisms which enhance the rate of interprotein transfer based on specific effects occurring on complex formation. For example, it has been suggested that the outer-sphere reorganization energy term is reduced significantly upon complex formation due to solvent exclusion at the interface between solvent exposed cofactors (hemes) (*48*). Although as indicated in the companions paper, this effect is likely to be small (*49*) but possibly still significant (i.e., given the exponential dependence of the rate on this term) as indicated below. It has also been suggested that the effective charge in the vicinity of the redox active center modulates the redox potential in a manner which favors electron transfer (*48*). The relatively slow rate of electron transfer may be due principally to a nonoptimal orientation of heme cofactors in the complex (*49*).

The sum of cytochrome b_5's reorganization energy and hemoglobin's reorganization energy is 1.2 eV which is 0.3 eV higher than McLendon's estimate based on the temperature dependence of the homogeneous phase rate constant (*23*). This difference alone accounts for a factor of 23 in the rate, bringing the calculated value for the homogeneous electron-transfer rate constant to 0.048 s^{-1}, which is a difference of only 30%. Thus, a reduction of only 0.15 eV in the outersphere term of the reorganization energy for each redox active protein due to solvent exclusion could account for the difference in calculated and measured rates.

CONCLUSIONS

We have shown the direct voltammetry of oxygen transport proteins using ω-hydroxyalkanethiol modified Au electrodes can be performed as easily as for small molecules. The reorganization energy and relative electronic coupling of hemoglobin and myoglobin are nearly identical. The redox Bohr effect illustrates functional allosteric intactness of hemoglobin and is in good agreement with previously published results. We have also shown that one can calculate the homogeneous electron transfer rate constant of a biologically important protein−protein interaction given the heterogeneous electron transfer rates of the individual components. The reasonable agreement between rates determined in homogeneous solution phase experiments employing stopped-flow methods and those calculated based on kinetics derived from heterogeneous electrode reactions suggests that the intrinsic electroreactivity of heme proteins is sufficient to account for physiologically relevant homogeneous phase rates, although there are indications that a reduction in the outer-sphere reoganization energy due to solvent exclusion on complex formation facilitates electron transfer.

REFERENCES

1. Becka, A. M., and Miller, C. J. (1992) *J. Phys. Chem. 96*, 2657−2668.
2. Terrettaz, S., Becka, A. M., Traub, M. J., Fettinger, J. C., and Miller, C. J. (1995) *J. Phys. Chem. 99*, 11216−11224.
3. Cheng, J., Saghi-Szab, G., Tossell, J., and Miller, C. J. (1996) *J. Am. Chem. Soc. 118*, 680−684.
4. Terrettaz, S., Cheng, J., Miller, C. J., and Guiles, R. D. (1996) *J. Am. Chem. Soc. 118*, 7857−7858.
5. Cheng, J., Terrettaz, S., Blankman, J. I., Miller, C. J., Dangi, B., and Guiles, R. D. (1997) *Isr. J. Chem. 37*, 259−266.
6. Ye, J., and Baldwin, R. P. (1988) *Anal. Chem. 60*, 2263−2268.
7. Song, S., and Dong, S.(1988) *Bioelectrochem. Bioenerg. 19*, 337−346.
8. Ciureanu, M., Goldstein, S., and Mateescu, M. A. (1998) *J. Electrochem. Soc. 145*, 533−541.
9. Chen, X., Hu, N., Zeng, Y., Rusling, J. F., and Yang, J. (1999) *Langmuir 15*, 7022−7030.
10. Zhang, S., Sun, W.-L., Zhang, W., Jin, L.-T., Yamamoto, K., Tao, S., and Jin, J. (1998) *Anal. Lett. 31*, 2159−2171.
11. Li, G., Fang, H., and Zu, D. (1996) *Anal. Lett. 29*, 1273−1277.
12. Becka, A. M., and Miller, C. J. (1993) *J. Phys. Chem. 97*, 6233−6239.
13. Bunn, H. F., and Forget, B. G. (1986) *Hemoglobin: Molecular, Genetic and Clinical Aspects*, W. B. Saunders Company, Philadelphia.
14. Papa, S., Guerrieri, F., and Izzo, G. (1986) in *Cooperative Proton-Transfer Reactions in the Respiratory Chain: Redox Bohr Effects* (Fleischer, S., and Fleischer, B., Ed.) Vol. 126, pp 331−343, Academic Press, Inc., New York.
15. Tarlov, M. J., and Bowden, E. F. (1991) *J. Am. Chem. Soc. 113*, 1847−1849.
16. Eddowes, M. J., and Hill, H. A. O. (1982) *Faraday Discuss. Chem. Soc. 74*, 331−341.
17. Castner, J. F., and Hawdridge, F. M. (1983) *J. Electroanal. Chem. 143*, 217−232.
18. Reed, D. E., and Hawkridge, F. M. (1987) *Anal. Chem. 59*, 2334−2339.
19. Szücs, A., and Novák, M. (1995) *J. Electroanal. Chem. 383*, 75−84.
20. Weaver, M. J. (1976) *Inorg. Chem. 15*, 1733−1735.
21. Weaver, M. J. (1980) *J. Phys. Chem. 84*, 568−576.
22. Weaver, M. J. (1990) *J. Phys. Chem. 94*, 8608−8613.
23. Qiao, T., Simmons, J., Horn, D. A., Chandler, R., and McLendon, G. (1993) *J. Phys. Chem. 97*, 13089−13091.
24. Marcus, R. A. (1965) *J. Chem. Phys. 43*, 679−701.
25. Marcus, R. A., and Sutin, N. (1985) *Biochim. Biophys. Acta 811*, 265−322.
26. Sarma, S., DiGate, R. J., Goodin, D. B., Miller, C. J., and Guiles, R. D. (1997) *Biochemistry 36*, 5658−5668.
27. Dangi, B., Blankman, J. I., Miller, C. J., Volkman, B. F., and Guiles, R. D. (1998) *J. Phys. Chem. B 102*, 8201−8208.
28. Faulkner, K. M., Bonaventura, C., and Crumbliss, A. L. (1994) *Inorg. Chim. Acta 226*, 187−194.
29. Faulkner, K. M., Bonaventura, C., and Crumbliss, A. L. (1995) *J. Biol. Chem. 270*, 13604−13612.
30. Miller, C., and Grätzel, M. (1991) *J. Phys. Chem. 95*, 5225−5233.
31. Antonini, E., and Bunori, M. (1971) *Hemoglobin and Myoglobin in their reactions with ligands*, American Elsevier Publishing Co., New York.
32. King, B. C., Hawkridge, F. M., and Hoffman, B. M. (1992) *J. Am. Chem. Soc. 114*, 10603−10608.
33. Miller, C. J. (1995) in *Heterogeneous electron-transfer kinetics at metallic electrodes* (Rubinstein, I., Ed.) pp 27−79, Marcel-Dekker, New York.
34. Mauk, M. R., and Mauk, A.-G. (1982) *Biochemistry 21*, 4730−4734.
35. Naito, N. R., Huang, H., Sturgess, A. W., Nocek, J. M., and Hoffman, B. M. (1998) *J. Am. Chem. Soc. 120*, 11256−11262.
36. Perlmutter-Hayman, B. (1971) *Prog. React. Kinet. 6*, 239−267.
37. Frese, K. W., Jr. (1981) *J. Phys. Chem. 85*, 3911−3916.
38. Cummins, D., and Gray, H. B. (1977) *J. Am. Chem. Soc. 99*, 5158−5167.
39. Stonehuerner, J., Williams, J. B., and Millett, F. (1979) *Biochemistry 18*, 5422−5427.
40. Rosenberg, R. C., Wherland, S., Howerda, R. A., and Gray, H. B. (1976) *J. Am. Chem. Soc. 98*, 6364−6369.
41. Meyer, T. E., Watkins, J. A., Przysiecki, C. T., Tollin, G., Cusanovish, M. A. (1984) *Biochemistry 23*, 4761−4767.
42. Van Leeuwen, J. W., Mofers, F. J. M., and Veerman, E. C. I. (1981) *Biochim. Biophys. Acta 635*, 434−439.
43. Chien, J. C. W., Gibson, H. L., and Dickinson, L. C. (1978) *Biochemistry 17*, 2579−2584.
44. Holwerda, R. A., Knaff, D. B., Gray, H. B., Clemmer, J. D., Crowley, R., Smith, J. M., and Mauk, A. G. (1980) *J. Am. Chem. Soc. 102*, 1142−1146.
45. Brönsted, J. N. (1922) *J. Am. Chem. Soc. 44*, 877−898.
46. Dickerson, R. E., and Geis, I. (1983) *Hemoglobin: Structure, Function, Evolution, and Pathology*, Benjamin/Cummings Publishing Company, Inc., Reading.
47. Langridge, R., Ferrin, T. E., Kuntz, I. D., and Connolly, M. L. (1981) *Science 211*, 661−666.
48. Zhou, H.-X. (1994) *J. Am. Chem. Soc. 116*, 10362−10375.
49. Blankman, J. I., Shahzad, N., Dangi. B., Miller, C. J., and Guiles, R. D. (2000) *Biochemistry 39*, 14799−14805.

BI000731B